A comprehensive analysis on radiation shielding characteristics of borogypsum (boron waste) by Phy-X/PSD code

M. Aygun[a] and Z. Aygun[b]

[a]*Department of Physics, Bitlis Eren University, Bitlis, Turkey.*
[b]*Vocational School of Technical Sciences, Bitlis Eren University, Bitlis, Turkey.*

Received 14 March 2022; accepted 21 December 2022

In the present study, radiation shielding characteristics of the borogypsum, which is a waste generated during the boric acid production in Turkey, was analyzed. For this purpose, we used recently developed Phy-X/PSD software, which is provided to calculate shielding parameters such as mass attenuation coefficient, linear attenuation coefficient, half-value layer, tenth-value layer, effective atomic number, total atomic cross section, total electronic cross section, effective conductivity, effective electron number, buildup factors and fast neutron removal cross section in a wide photon energy range. Additionally, mass attenuation coefficients of borogypsum were compared with those of other radiation shielding materials (ordinary concrete, obsidian, pumice, clay) in order to give a significant evaluation about the radiation shielding capability of borogypsum. Half value layer and fast neutron removal cross section values are also evaluated by other materials. It is noticed that borogypsum has higher shielding potential than other reported shielding materials.

Keywords: Phy-X/PSD; radiation attenuation parameters; borogypsum.

DOI: https://doi.org/10.31349/RevMexFis.69.040401

1. Introduction

Development of modern technology increases the radiation applications in our daily lives. This increase makes it necessary the protection from the harms of radiation. Therefore, it becomes significant to search alternative shielding materials. The waste materials can be used as shielding materials in order to reduce waste disposal costs and protect non-renewable resources.

The recycling of the waste produced by the sectors as an alternative raw material is successfully carried out in many countries for a long time. The reasons that lead countries to this can be listed as depletion of natural resources; conservation of non-renewable resources; improving population health and safety; reduction in waste disposal costs. Natural resources are important for the development of countries and a strong relationship is existing between the use of natural resources and economic development. One of the most important natural sources is boron which is commonly used in different areas such as energy, medicine, and industry. Boron reserves of Turkey correspond to ≈72% of the World [1]. Colemanite, tincal and ulexite are the commercial boron ores of Turkey. Reaction of colemanite with sulphuric acid produces boric acid, and borogypsum (BG) is the waste which is formed by the production of boric acid [2].

There are many researches in the literature about the use of BG as a cement additive [3–5], as a cement replacement in mortar production [6,7]. The leaching kinetics [8–10] and the strength properties [1] of BG were also reported before. Mass attenuation coefficients measured at 59.54 and 80.99 keV of concrete samples including BG and colemanite were studied by Demir and Keleş [11]. Celen *et al.* [12] studied the linear attenuation coefficient of BG-barite composition at 662, 1173 and 1332 keV. The linear attenuation coefficients obtained at the photon energies of 662, 1173 and 1332 keV of panels containing BG produced with mineral additives were determined by Celen and Evcin [13]. However, to the best of our knowledge, there is not any detailed study about all the photon attenuation parameters of BG in a wide energy range in the literature. The performance of a radiation shielding material can be identified by determining radiation-matter interaction parameters comprehensively.

In this study, the photon attenuation parameters such as atomic and electronic cross sections (ACS and ECS), mass attenuation coefficients (MAC), linear attenuation coefficients (LAC), mean free paths (MFP), half-value layer (HVL), tenth-value layer (TVL), effective atomic numbers (Zeff), electron densities (Neff), effective conductivity (Ceff), buildup factors (EBF and EABF) and fast neutron removal cross section (FNRCS) of the boron waste, BG, were determined. For the purpose of having knowledge about the radiation shielding capability of the sample, recently developed code Phy-X/PSD [14] was applied. Phy-X/PSD software is recently used to determine the radiation shielding parameters of different materials. Calculation process is started by inserting the density and chemical composition of the material which can be entered as mole fraction or weight fraction. The parameters are determined in a wide energy range of 1 keV-100 GeV by selecting the energy sources.

2. Material and calculation process

In the study, we used the density value (2.41 g/cm^3) and the chemical composition of the BG obtained from the literature reported by Kunt *et al.* [2] to calculate the photon attenuation parameters of the sample. The parameters obtained in

calculation process by the codes are given with their formulas below.

The MAC can be calculated by the Beer-Lambert formulated as [14]:

$$I = I_0 e^{-\mu t}, \tag{1}$$

$$\mu_m = \frac{\mu}{\rho} = \frac{\ln(I_0/I)}{\rho t} = \frac{\ln(I_0/I)}{t_m}, \tag{2}$$

where I_0 and I are incident and attenuated photon intensities, ρ (g/cm^3) is the density of material, μ_m(cm^2/g) and μ(cm^{-1}) are mass and linear attenuation coefficients, t_m (g/cm^2) and t (cm) are sample mass thickness (the mass per unit area) and the thickness, respectively.

If the sample has various elements, we can write the total MAC for any compound as follows [14];

$$\frac{\mu}{\rho} = \sum_i w_i (\mu/\rho)_i, \tag{3}$$

where w_i and $(\mu/\rho)_i$ are the weight fraction and the mass attenuation coefficient of the ith constituent element, respectively.

ACS (σ_a) for any sample can be obtained by using the equation formulated as;

$$ACS = \sigma_a = \frac{N}{N_A}(\mu/\rho), \tag{4}$$

where N_A and N respectively are the Avogadro's number and the atomic mass of materials.

ECS (σ_e) is formulated by the following equation [15];

$$ECS = \sigma_e = \frac{\sigma_a}{Z_{\text{eff}}}. \tag{5}$$

By using the Eqs. (4) and (5) Z_{eff} of the material can be found as follows;

$$Z_{\text{eff}} = \frac{\sigma_a}{\sigma_e}. \tag{6}$$

We can calculate N_{eff}, as follows [16],

$$N_{\text{eff}} = \frac{\mu_m}{\sigma_e}. \tag{7}$$

HVL and TVL are the thickness related parameters used in determining any radiation attenuation material by halving and one tenth the photon intensity, respectively. MFP is the average distance at which a photon travels through the material between two interactions. The μ is used to obtain the parameters given by

$$HVL = \frac{\ln(2)}{\mu}, \tag{8}$$

$$MFP = \frac{1}{\mu}, \tag{9}$$

$$TVL = \frac{\ln(10)}{\mu}, \tag{10}$$

C_{eff} of materials can be given by the following equation [17]:

$$C_{\text{eff}} = \left(\frac{N_{\text{eff}}\, \rho e^2 \tau}{m_e}\right) 10^3, \tag{11}$$

where m_e (kg) and $e(C)$ are mass and charge of electron, respectively.

FNRCS ($\sum R$) values of the materials can be obtained with the following equation [18, 19]:

$$\sum R = \sum_i \rho_i \left(\frac{\sum R}{\rho}\right)_i, \tag{12}$$

where $(\sum R/\rho)_i$ is the mass removal cross-section of the i^{th} constituent element and ρ_i is the partial density of the material.

For determination of energy absorption buildup factors (EABF) or exposure buildup factors (EBF), the formulas given below are used. The ratio R of Compton partial mass attenuation coefficient to total mass attenuation coefficient must be defined for the material at certain energy. The R value obtained for the material must be between the (μ_m)Compton/(μ_m)Total values calculated for the two adjacent elements. The R_1 and R_2 values denote the (μ_m) Compton/(μ_m) Total ratios of these two adjacent elements which have Z_1 and Z_2 atomic numbers. F is the geometric progression (G-P) fitting parameters (a, b, c, d, X_K coefficients) of the studied material. F_1 and F_2 are the values of G-P fitting parameters corresponding to the Z_1 and Z_2 atomic numbers at a certain energy, respectively. E and X denote primary photon energy and penetration depth, respectively. Combination of $K(E, X)$ with X, performs the photon dose multiplication and determines the shape of the spectrum [20–22].

$$Z_{eq} = \frac{Z_1(\log R_2 - \log R) + Z_2(\log R - \log R_1)}{\log R_2 - \log R_1}, \tag{13}$$

$$F = \frac{F_1(\log Z_2 - \log Z_{eq}) + F_2(\log Z_{eq} - \log Z_1)}{\log Z_2 - \log Z_1}, \tag{14}$$

$$B(E,x) = 1 + \frac{(b-1)(K^x - 1)}{(K-1)} \quad \text{for} \quad K \neq 1, \tag{15}$$

$$B(E,x) = 1 + (b-1)x \ \text{ for } \ K = 1, \tag{16}$$

$$K(E,x) = cx^a + d\frac{\tanh(\frac{x}{x_k} - 2) - \tanh(-2)}{1 - \tanh(-2)}$$

$$\text{for } \ x \leq 40 \ \text{ mfp (cm)}. \tag{17}$$

3. Results and discussion

The chemical composition of BG, which is given by Kunt *et al.* [2], is shown in Table I. Variation of the calculated MAC values by Phy-X/PSD of BG versus photon energies is given in Fig. 1. In order to verify the validity of the Phy-X/PSD program, the MAC values of BG are also calculated by XCom [23] and a good agreement is obtained by both of

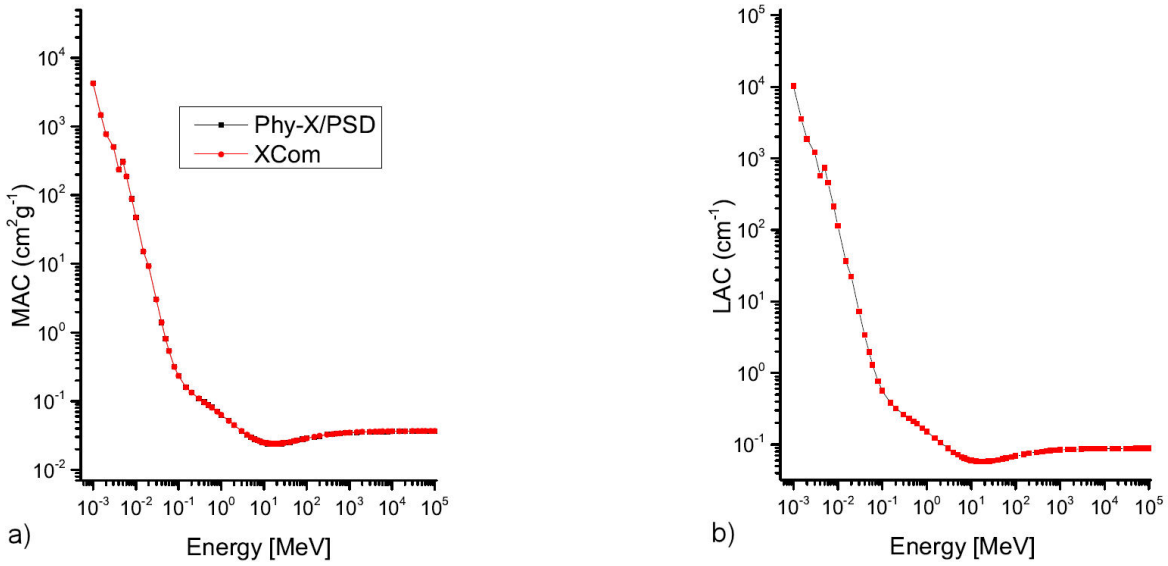

FIGURE 1. The dependence of MAC a) and LAC b) values on incident photon energies.

the codes. The XCom is a database for determining MAC values for multi-element materials. It uses interpolations of the elemental MAC values or elemental cross-sections at certain energies and applies the mixture rule based on the specified compositions. Total MAC values are interpolated by XCom using a log-log cubic spline fit [24]. XCom software is widely used to calculate the MAC values of elements, compounds, or mixtures in the energy range 1 keV-100 GeV. The other radiation protection parameters (LAC, HVL, MFP etc.) cannot be determined by the XCOM, while recently developed online software, Phy-X/PSD, can be used for the calculation of radiation-matter interaction parameters (LAC, MAC, HVL, MFP, TVL, Zeff, Neff, EABF, EBF) in the energy region of 1 keV-100 GeV. The Phy-X/PSD program, a WinXCom based software, makes an evaluation by using XCOM-NIST photoatomic library. It gives the output data in the form of an excel data sheet [25]. At low energies (1-100 keV) where the photoelectric process is predominant, MAC values decreased sharply with increasing energy. At intermediate energies

TABLE I. Chemical composition of BG.

Compounds	%wt
SO_3	45.9
K_2O	0.55
CaO	46
Sc_2O_3	0.64
Fe_2O_3	1.1
CuO	0.07
As_2O_3	0.22
SrO	5.48
ZrO_2	0.01
PbO	0.03

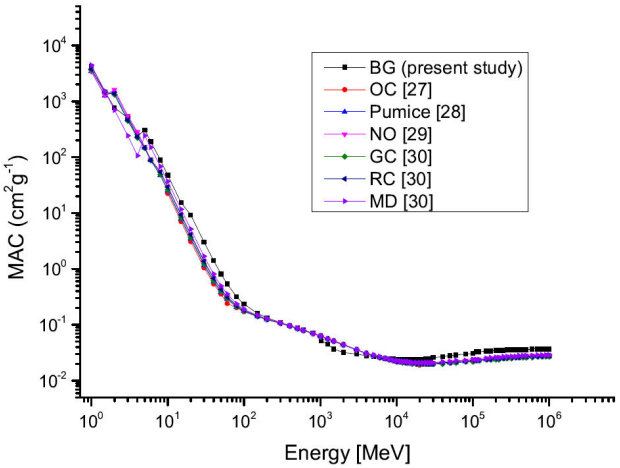

FIGURE 2. MAC values of BG and other shielding materials.

(100 keV-5 MeV) where the Compton scattering is dominant, MAC values slightly changed. Above 5 MeV, the Pair production process starts and MAC values increased with increasing energy [26]. Additionally, we compared the MAC values of BG with those of other reported shielding materials, ordinary concrete (OC), green clay (GC), red clay (RC), pumice, Nemrut obsidian (NO), marble dust (MD) [27–30] (Fig. 2). As a result of the comparison of obtained MAC values for BG with those for the other materials, it can be concluded that the shielding potential of BG is higher than those. LAC is a considerable parameter for defining the photon-matter interaction. The value of LAC depends on both MAC and density of sample. LAC values are greater than MAC values due to the density effect (Fig. 1).

The HVL and TVL parameters give the information about the penetration ability of the radiations in materials. MFP is the average distance taken by photon in the material between

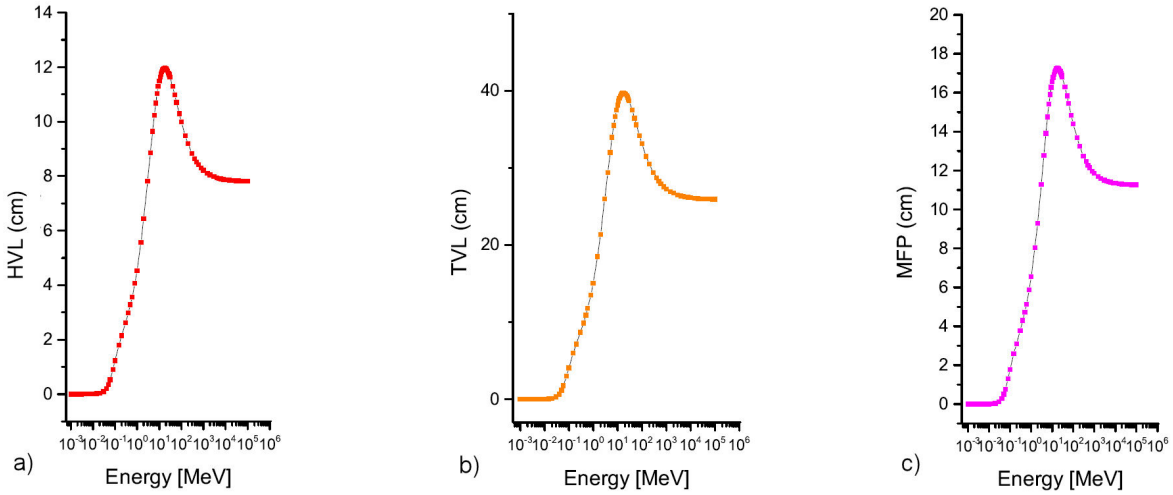

FIGURE 3. The dependence of HVL a) TVL b) MFP c) values on incident photon energies.

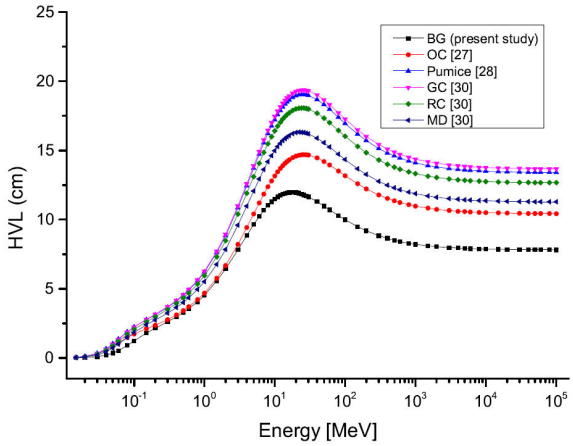

FIGURE 4. HVL values of BG and other shielding materials.

two collisions. The change of HVL, TVL and MFP values versus photon energies is given in Fig. 3. Compton scattering region (at mid-energies), most photons are more likely to be scattered. Therefore, they have lower absorption probabilities, and hence thicker materials and longer MFP values are required. Furthermore, HVL values of BG are compared with other materials in order to see the thickness advantage of the boron waste for shielding ability (Fig. 4). BG has lower HVL values than the others in a wide energy range as a shielding material.

The interaction possibility of per atom and per electron in a unit volume of any material is given by ACS and ECS, respectively. ACS and ECS values change with incident photon energies as given in Fig. 5. The ACS and ECS values of BG decrease proportionally with increasing photon energy

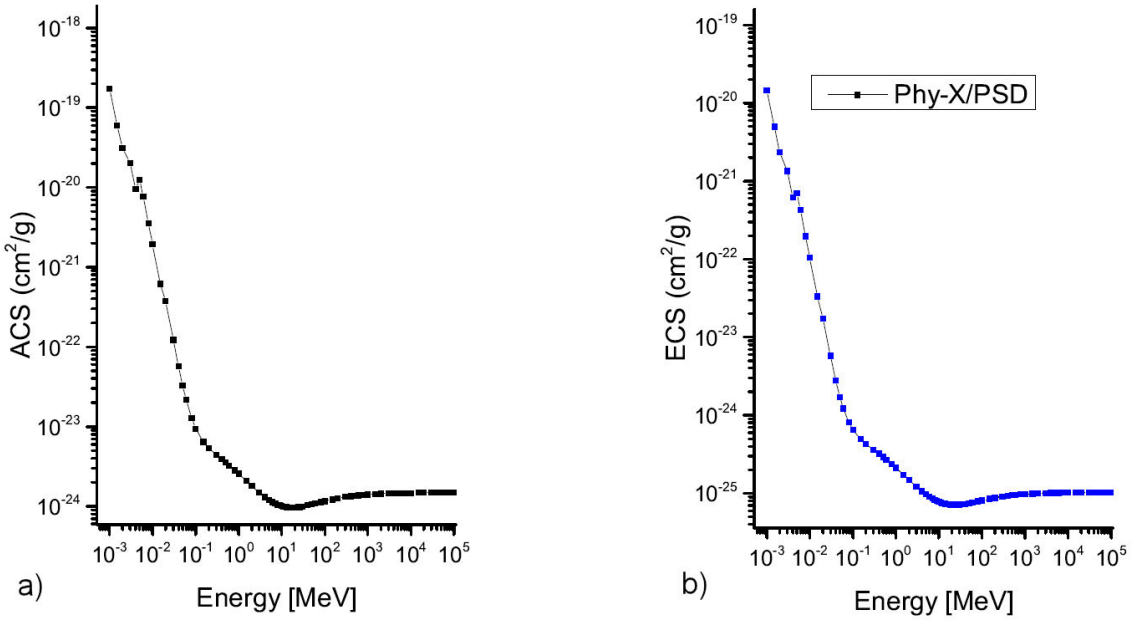

FIGURE 5. The dependence of ACS a) and ECS b) values on incident photon energies.

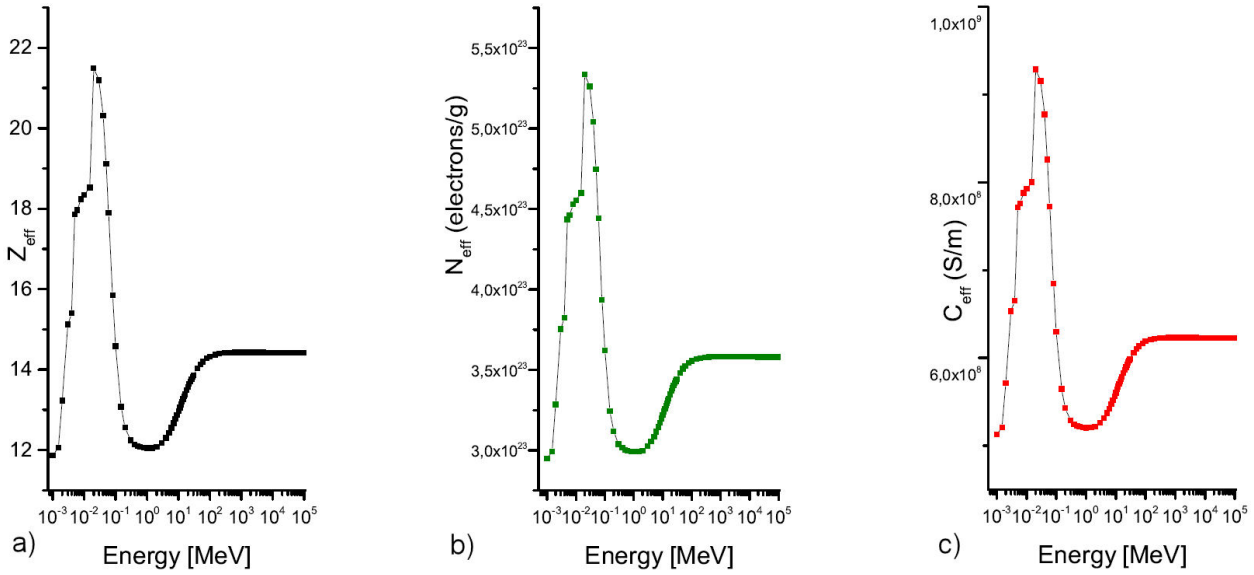

FIGURE 6. The dependence of Z_{eff} a) N_{eff} b) C_{eff} c) values on incident photon energies.

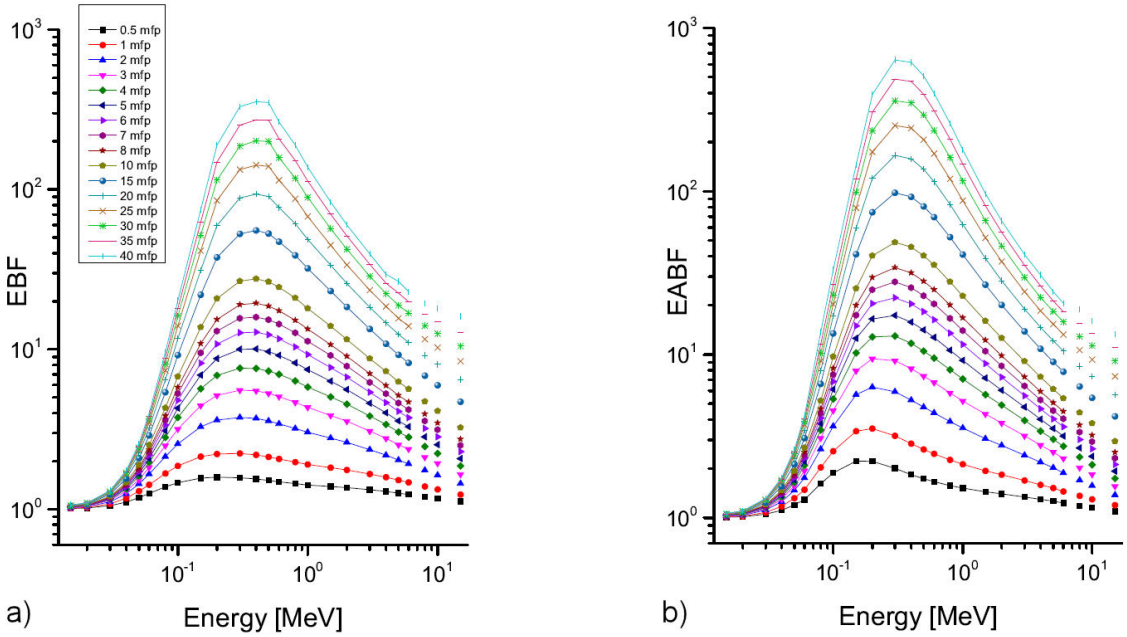

FIGURE 7. The dependence of EBF a) and EABF b) values on incident photon energies.

due to the decrease in the probability of photon-atom interaction.

The energy dependence of Z_{eff}, C_{eff} and N_{eff} values is given in Fig. 6. In photoelectric effect region (at low energies), maximum Z_{eff} values were obtained varied with Z^{4-5}. By increasing energy, these values decreased sharply with $E^{-3.5}$. Then the values gradually increased and stayed constant at high energies by pair production varied with Z^2. Z_{eff} values of the samples generally depend on the atomic numbers of the elements in the compositions. It is obvious that the increase of the Z_{eff} value is due to the presence of Pb content in the sample. N_{eff} is the parameter that represents the effective conductivity of the compound [31]. As shown in Fig. 6, the variation of the N_{eff} values on the incident photon energies is similar with the variation of Z_{eff} values. The larger effective atomic number causes the interaction between the photons and more free electrons [32]. Interactions (photoelectric effect, Compton scattering, and pair production) between photons and material changes the number of free electrons in the material. This causes changes of C_{eff} values and dependence of C_{eff} on photon energies is seen in Fig. 6.

The change of EBF and EABF versus incident photon energies is shown in Fig. 7. Buildup factor values are small at low energies as a result of the photoelectric effect. EBF and EABF reach the maximum values at mid-energies due to the large number of scattered photons in consequence of Comp-

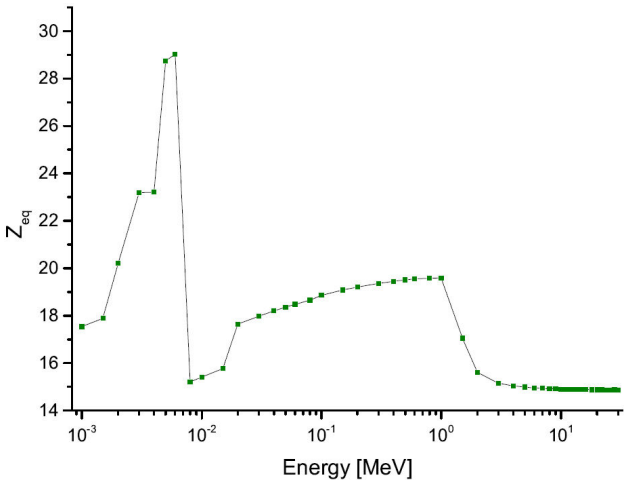

FIGURE 8. The dependence of Z_{eq} on incident photon energies.

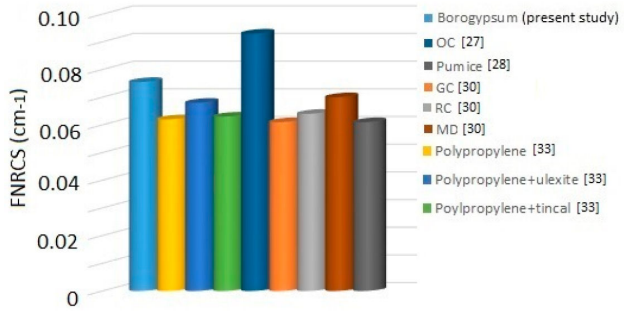

FIGURE 9. FNRCS values of BG and other shielding materials.

ton effect. At high energies, pair production is the effective process, therefore photon absorption is observed strongly and a decrease in buildup factors is observed in this region [29, 30]. It can be said that the buildup effect is predominant in the mid-energy region. The probability of photon scattering increases with increasing penetration depth, and so EBF and EABF values achieve high values at higher MFP values.

Equivalent atomic number (Z_{eq}) is the parameter on determination of energy absorption calculation and absorbed dose. Z_{eq} is affected only by Compton scattering [29, 30]. The change of calculated Z_{eq} of BG is given in Fig. 8. Z_{eq} values with energy-dependent fluctuations are observed for materials which are composed of many elements with large differences in atomic numbers as seen for Z_{eff}, N_{eff} and C_{eff} parameters.

Fast neutron attenuation abilities of the sample are also determined by Phy-X/PSD. Fast neutron removal cross section (FNRCS) value of BG is 0.076. The comparison for FNRCS values of BG and different samples reported previously [27, 28, 30, 33] are given in Fig. 9. It is obtained that BG has higher neutron attenuation after OC among the given shielding materials.

4. Conclusions

In the paper, we investigated the radiation shielding potential of BG by determination of photon attenuation parameters in the energy range of 1keV-100GeV. For this purpose, Phy-X/PSD software was used. Depending on comparison of obtained MAC values of BG with those of other shielding materials (OC, GC, RC, pumice, MD, NO), it can be stated that the shielding potential of BG is higher than those. It is obvious that Z_{eff} value is mainly depend on the composition of the sample. Having elements with high atomic numbers such as Pb, Sr, Zr make the parameter higher. Z_{eq} values have energy-dependent fluctuations due to the presence of many elements with large differences in atomic numbers as seen for Z_{eff}, N_{eff} and C_{eff} parameters. Additionally, FNRCS value of BG enables to evaluate the sample as an appropriate neutron shielded.

1. U.K. Sevim, Y. Tumen, *Strength and fresh properties of borogypsum concrete*, Construct. Building. Mater. **48** (2013) 342-347. https://doi.org/10.1016/j.conbuildmat.2013.06.054.
2. K. Kunt, F. Dur, B. Ertinmaz, M. Yildirim, E.M. Derun, S. Piskin, *Utilization of Boron Waste as an Additive for Cement Production*, CBU J. Sci. **11** (2015) 383-389.
3. R. Boncukoglu, T.M. Yılmaz, M.M. Kocakerim, V. Tosunoglu, *Utilization of borogypsum as set retarder in Portland cement production*, Cem. Concr. Res. **32** (2002) 471-5. https://doi.org/10.1016/S0008-8846(01)00711-6.
4. I.F. Elbeyli, E.M. Derun, J. Gulen, S. Piskin, *Thermal analysis of borogypsum and its effects on the physical properties of Portland cement*, Cem. Concr. Res. **33** (2003) 1729-1735. https://doi.org/10.1016/S0008-8846(03)00110-8.
5. Y. Erdogan, H. Genc, A. Demirbas, *Utilization of borogypsum for cement*, Cem. Concr. Res. **22** (1992) 841-4. https://doi.org/10.1016/0008-8846(92)90108-8.
6. T. Kavas, A. Olgun, Y. Erdogan, *Setting and hardening of borogypsum-Portland cement clinker-fly ash blends. Studies on effects of molasses on properties of mortar containing borogypsum*, Cem. Concr. Res. **35** (2005) 711-8. https://doi.org/10.1016/j.cemconres.2004.05.019.
7. A. Demirbas, S. Karslıoglu, *The effect of boric acid sludges containing borogypsum on properties of cement*, Cem. Concr. Res. **25** (1995) 1381-4. https://doi.org/10.1016/0008-8846(95)00130-5.
8. A. Demirbas, *Recyciling of lithium from borogypsum by leaching with water and leaching kinetics*, Resour. Conserv. Recycling **25** (1999) 125-31.
9. A. Demirbas, H. Yuksek, I. Cakmak, M.M. Kucuk, M. Cengiz, M. Alkan, *Recovery of boric acid from boronic wastes by leaching with water, carbon dioxide- or sulfur dioxide-*

saturated water and leaching kinetics, Resour. Conserv. Recycling **28** (2000) 135-146. https://doi.org/10.1016/S0921-3449(99)00039-7.

10. I. Alp, H. Deveci, Y.H. Sungun, E.Y. Yazici, M. Savas, S. Demirci, *Leachable characteristics of arsenical borogypsum wastes and their potential use in cement production*, Environ. Sci. Technol. **43** (2009) 6939-43. https://doi.org/10.1021/es9013008.

11. D. Demir, G. Keles. *Radiation transmission of concrete including boron waste for 59.54 and 80.99 keV gamma rays*. Nucl. Instr. Methods B **6** (2006) 501-4. https://doi.org/10.1016/j.nimb.2005.11.139.

12. Y. Y. Çelen, A. Evcin, I. Akkurt, N. Ç. Bezir, K. Günoğlu, N. Kutu, *Evaluation of boron waste and barite against radiation*, Inter. J. Environmental Sci. Tech. **16** (2019) 5267-5274. https://doi.org/10.1007/s13762-019-02333-3.

13. Y.Y. Celen, A. Evcin, *Synthesis and Characterizations of Magnetite-Borogypsum for Radiation Shielding*, Emerg. Mater. Res. **9** (2020) 1-7. https://doi.org/10.1680/jemmr.20.00098.

14. E. Sakar, Ö.F. Özpolat, B. Alım, M.I. Sayyed, M. Kurudirek, *Phy-X / PSD: Development of a user friendly online software for calculation of parameters relevant to radiation shielding and dosimetry*, Radiat. Phys. Chem. **166** (2020) 1-12. https://doi.org/10.1016/j.radphyschem.2019.108496.

15. I. Han, L. Demir, *Determination of mass attenuation coefficients, effective atomic and electron numbers for Cr, Fe and Ni alloys at different energies*, Nucl. Instr. Methods B **267** (2009) 3-8. https://doi.org/10.1016/j.nimb.2008.10.004.

16. I. Han, L. Demir, *Studies on effective atomic numbers, electron densities from mass attenuation coefficients in TixCo1-x and CoxCu1-x alloys*, Nucl. Instr. Methods B **267** (2009) 3505-3510. https://doi.org/10.1016/j.nimb.2009.08.022.

17. H.C. Manjunatha, *A study of gamma attenuation parameters in poly methyl methacrylate and Kapton*, Radiat. Phys. Chem. **137** (2017) 254-259. https://doi.org/10.1016/j.radphyschem.2016.01.024.

18. E. Sakar, *Determination of photon-shielding features and build-up factors of nickel-silver alloys*, Radiat. Phys. Chem. **172** (2020) 1-13. https://doi.org/10.1016/j.radphyschem.2020.108778.

19. J. Wood, *Computational methods in reactor shielding* 2013, Elsevier.

20. Y. Harima, *An historical review and current status of buildup factor calculations and applications*, Radiat. Phys. Chem. **41** (1993) 631-672.

21. Y. Harima, Y. Sakamoto, S. Tanaka, M. Kawai, *Validity of the geometric-progression formula in approximating gamma-ray buildup factors*, Nucl. Sci. Engineer. **94** (1986) 24-35.

22. ANSI/ANS 6.4.3. *Gamma-ray Attenuation Coefficients and Buildup Factors for Engineering Materials*. American Nucl Soc, La Grange Park, Illinois (1991).

23. M.J. Berger, J.H. Hubbell, *XCOM: Photon Cross Sections Database, Web Version 1.2*. National Institute of Standards and Technology Gaithersburg, MD, (1987) 20899, USA, available at. https://physics.nist.gov/xcom.

24. F.C. Hila, G.P. Dicen, A.M.V. Javier-Hila, A. Asuncion-Astronomo, N.R.D. Guillermo, R.V. Rallos, I.A. Navarrete, A.V. Amorsolo, *Determination of Photon Shielding Parameters for Soils in Mangrove Forests*, Philippine J. Sci. **150** (2021) 245-256.

25. A.H. Almuqrin, M.I. Sayyed, B. Albarzan, A.M.V. Javier-Hila, N. Alwadai, A. Kumar, *Mechanical and Gamma-Ray Interaction Studies of PbO-MoO3-Li2O-B2O3 Glass System for Shielding Applications in The Low Energy Region: A Theoretical Approach*, Appl. Sci. **11** (2021) 5538.

26. Z. Aygun, M. Aygun, *Evaluation of radiation shielding potentials of Ni-based alloys, Inconel-617 and Incoloy-800HT, candidates for high temperature applications especially for nuclear reactors, by EpiXS and Phy-X/PSD codes*, J. Polytech. in press (2022). https://doi.org/10.2339/politeknik.1004657.

27. I.I. Bashter, *Calculation of radiation attenuation coefficients for shielding concretes*, Annl. Nucl. Energy **24** (1997) 1389-1401.

28. Z. Aygun, M. Aygun. *A study on usability of Ahlat ignimbrites and pumice as radiation shielding materials, by using EpiXS code*, Inter. J. Environ. Sci. Tech. **19** (2022) 5675-5688. https://doi.org/10.1007/s13762-021-03530-9.

29. Z. Aygun, N. Yarbasi, M. Aygun, *Spectroscopic and radiation shielding features of Nemrut, Pasinler, Sarikamis and Ikizdere obsidians in Turkey: Experimental and theoretical study*, Ceramics Inter. **47** (2021) 34207-34217. https://doi.org/10.1016/j.ceramint.2021.08.330.

30. Z. Aygun, M. Aygun, N. Yarbasi, *A study on radiation shielding potentials of green and red clayey soils in Turkey reinforced with marble dust and waste tire*, J. New Results Sci. **10** (2021) 46-59. https://doi.org/10.54187/jnrs.986038.

31. B. Alım, *Determination of Radiation Protection Features of the Ag2O Doped Boro-Tellurite Glasses Using Phy-X / PSD Software*, J. Inst. Sci. Tech. **10** (2020) 202-213. https://doi.org/10.21597/jist.640027.

32. K. Wang, J. Hu, T. Chen, J. Tang, Y. Zhai, Y. Feng, Z. Zhao, H. Fan, K. Wang, *Radiation shielding properties of flexible liquid metal-GaIn alloy*, Prog. Nucl. Energy **135** (2021) 103696. https://doi.org/10.1016/j.pnucene.2021.103696.

33. I. Bilici, B. Aygün, C.U. Deniz, B. Oz, M.I. Sayyed, A. Karabulut, *Fabrication of novel neutron shielding materials: Polypropylene composites containing colemanite, tincal and ulexite*, Prog. Nucl. Energy **141** (2021) 103954. https://doi.org/10.1016/j.pnucene.2021.103954.